

Supplementary Materials

Introducing carbon dots to NiFe LDH via mild coprecipitation-ageing method to construct heterojunction for effective oxygen evolution

*Zi-Ye Liu, Qian-Yu Wang, Ji-Ming Hu**

Department of Chemistry, Zhejiang University, Hangzhou 310027, P. R. China

*: Corresponding author. E-mail: kejmhu@zju.edu.cn. Tel: +86-571-87953297. Fax: +86-571-87951895.

Supplementary data

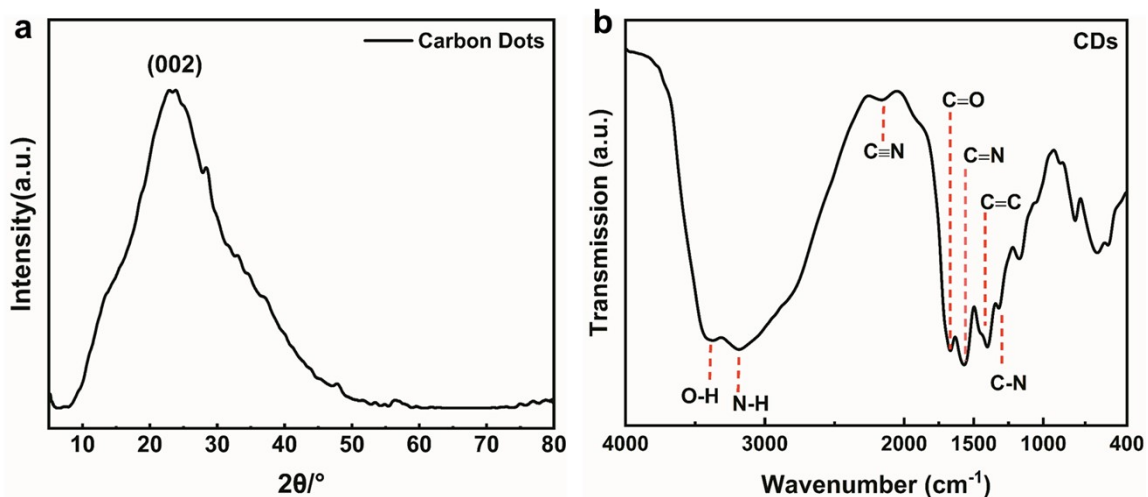


Fig. S1. (a) FTIR spectrum and (b) XRD pattern and of carbon dots

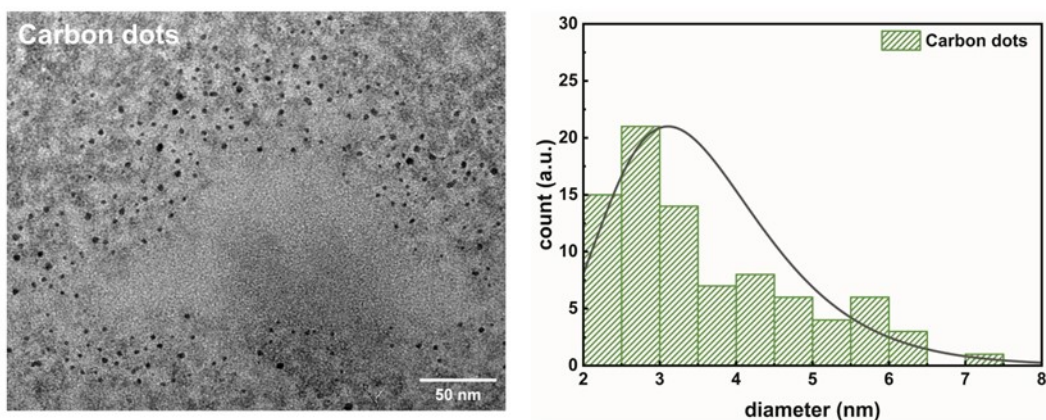


Fig. S2. TEM images and particle size distribution diagram of carbon dots.

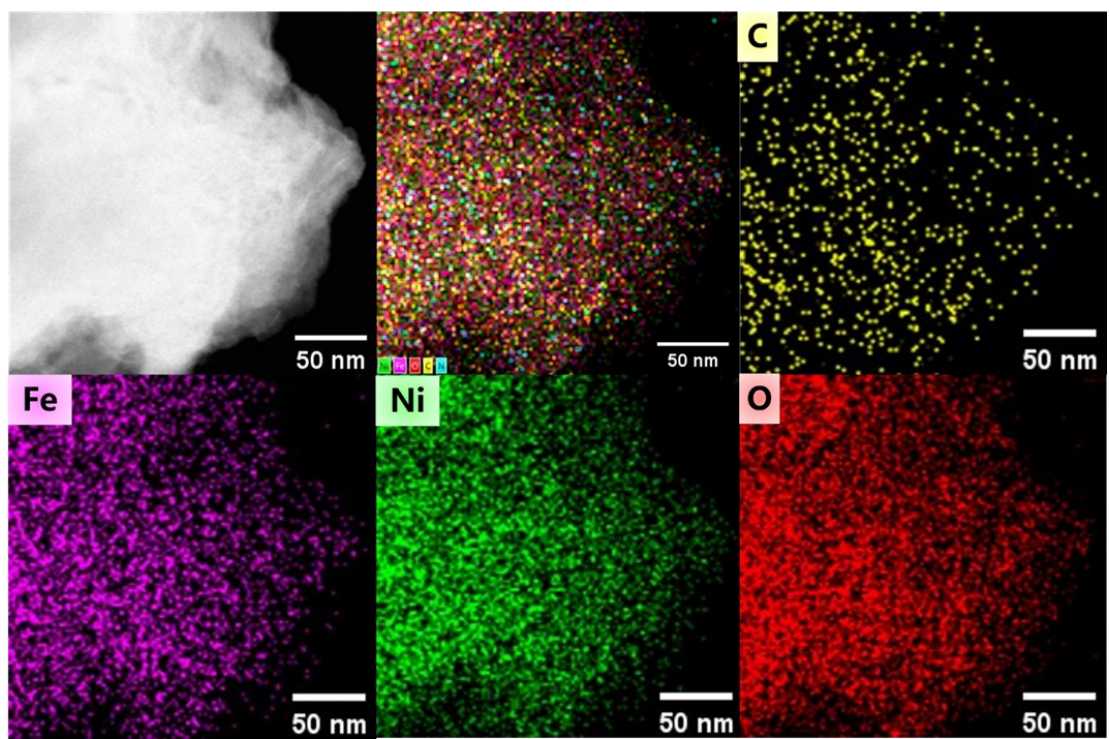


Fig. S3. Element mapping images of NiFe LDH

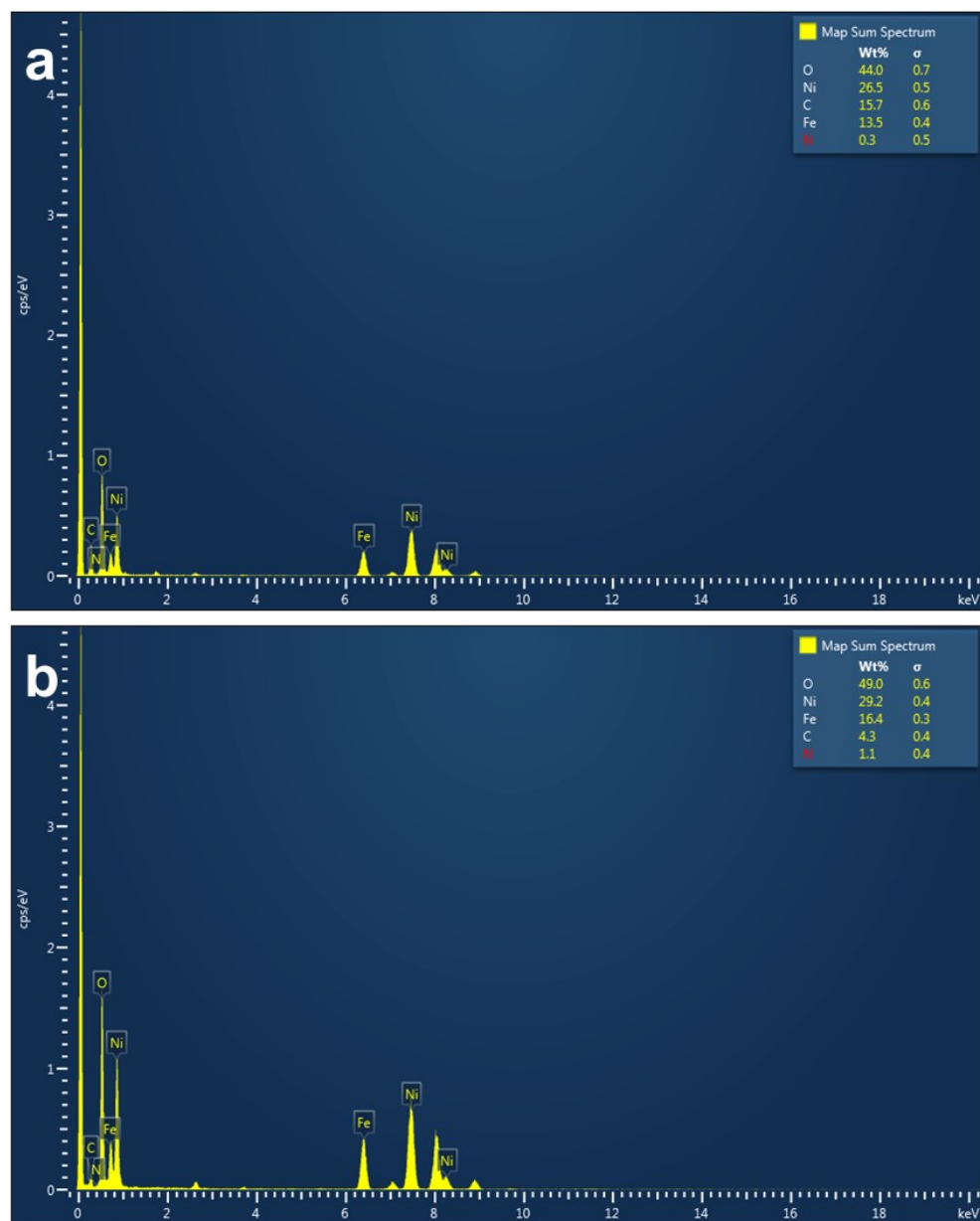


Fig. S4. EDS spectra of (a) NiFe LDH and (b) NiFe LDH@CDS-200.

Tab. S1. Elemental analysis of NiFe LDH, NiFe LDH@CDs-50, NiFe LDH@CDs-100, NiFe LDH@CDs-200 and carbon dots

Name	Weight [mg]	N [%]	C [%]	H [%]
NiFe LDH	1.887	0.34	1.58	3.26
NiFe LDH	1.937	0.47	1.56	3.13
NiFe LDH@CDs-50	1.986	0.65	2.37	2.97
NiFe LDH@CDs-50	1.859	0.65	2.36	2.93
NiFe LDH@CDs-100	1.988	0.34	2.67	3.03
NiFe LDH@CDs-100	1.918	0.36	2.64	3.02
NiFe LDH@CDs-200	1.851	0.22	3.11	3.10
NiFe LDH@CDs-200	1.857	0.23	3.14	3.08
CDs	1.979	21.22	36.95	6.23
CDs	1.960	20.95	36.58	6.38

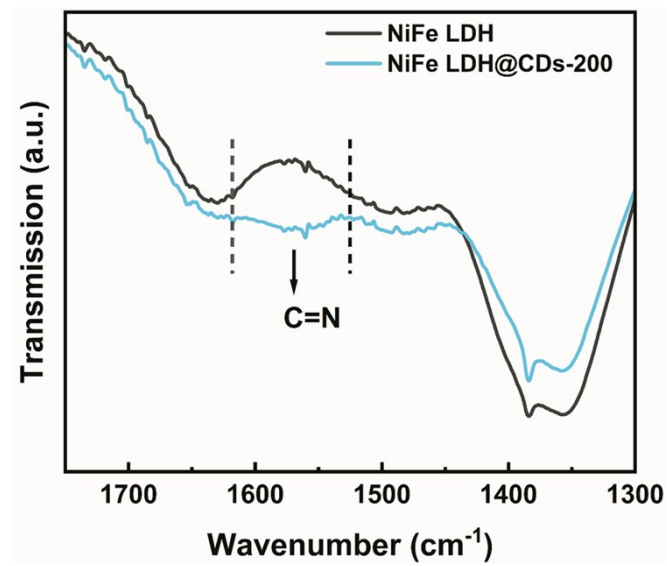


Fig. S5. FTIR spectra of NiFe LDH and NiFe LDH@CDs-200 ranging from 1300 cm^{-1} to 1730 cm^{-1} .

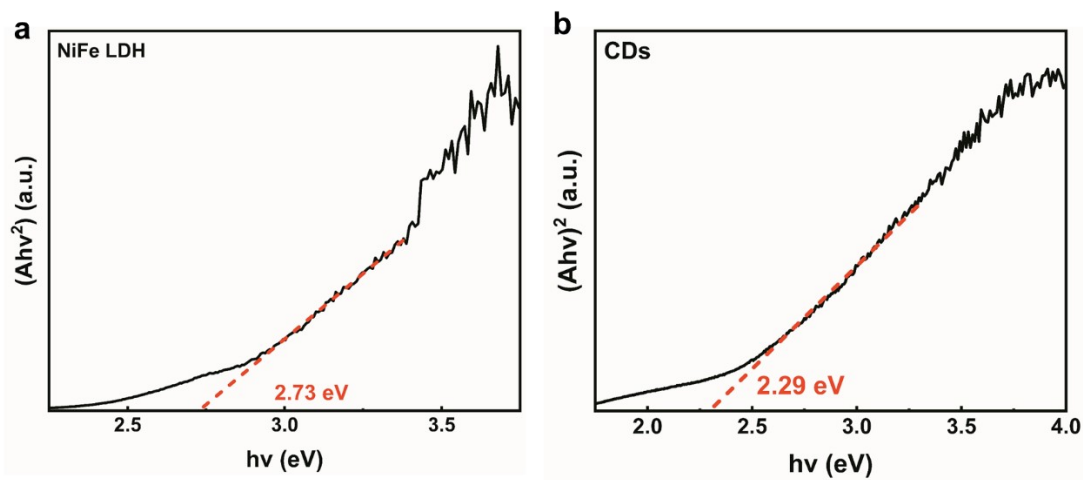


Fig. S6. Tauc plots of (a) NiFe LDH and (b) carbon dots.

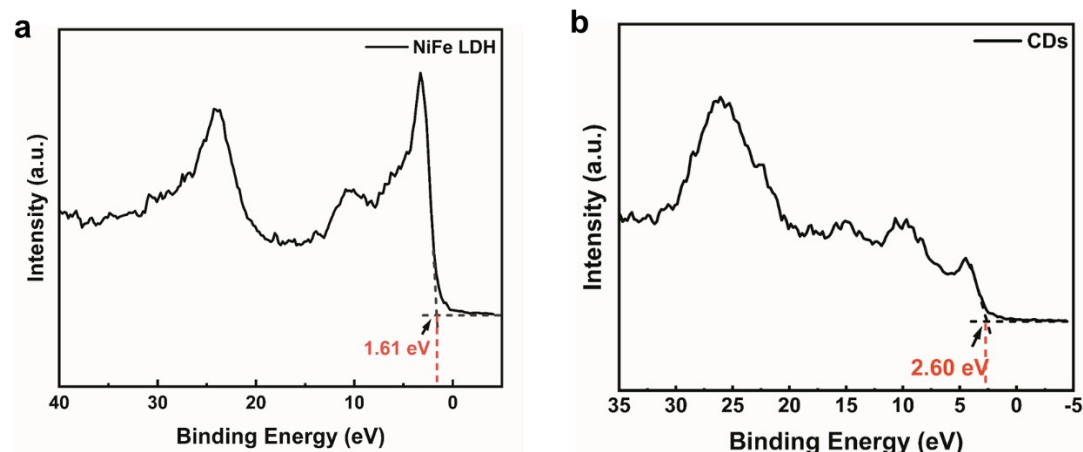


Fig. S7. VB-XPS spectra of (a) NiFe LDH and (b) carbon dots.

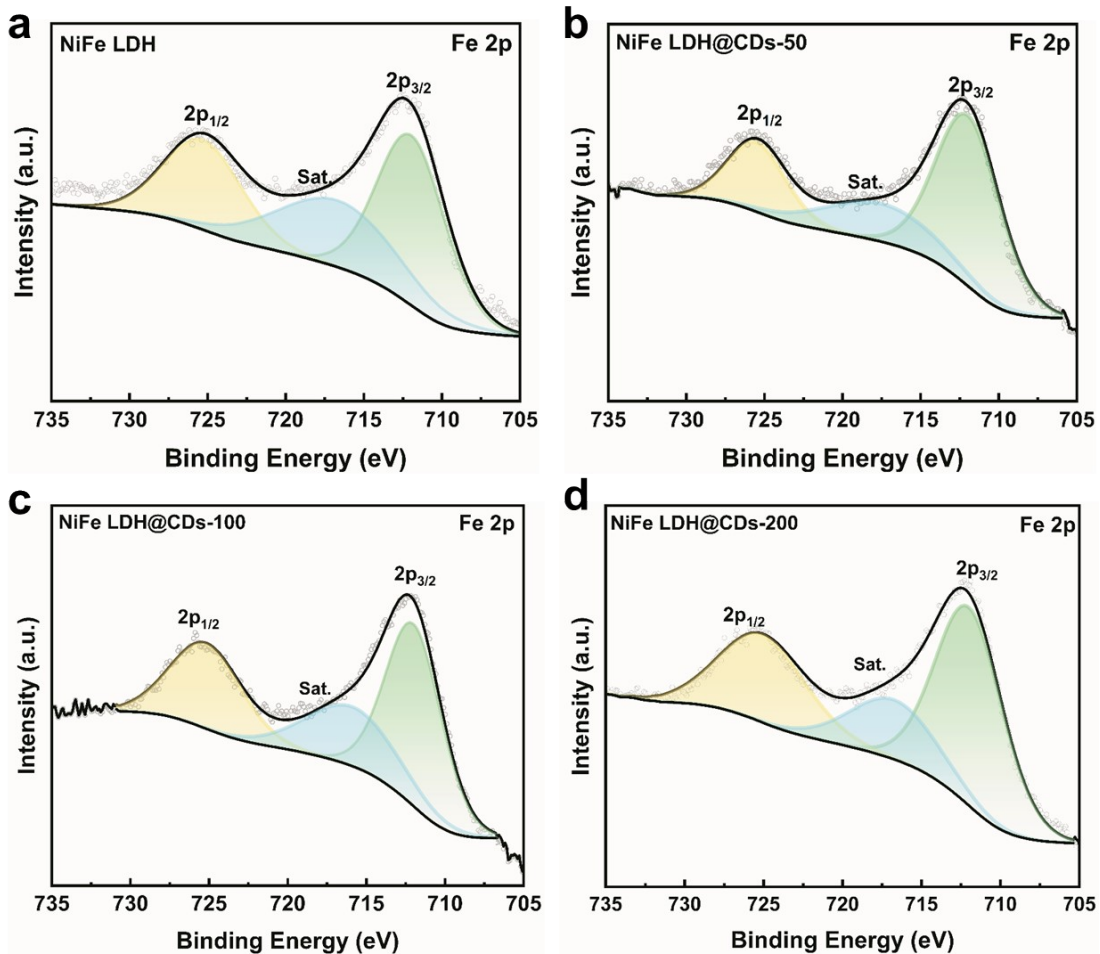


Fig. S8. Fe 2p XPS spectra of NiFe LDH (a), NiFe LDH@CDs-50 (b), NiFe LDH@CDs-100 (c) and NiFe LDH@CDs-200(d).

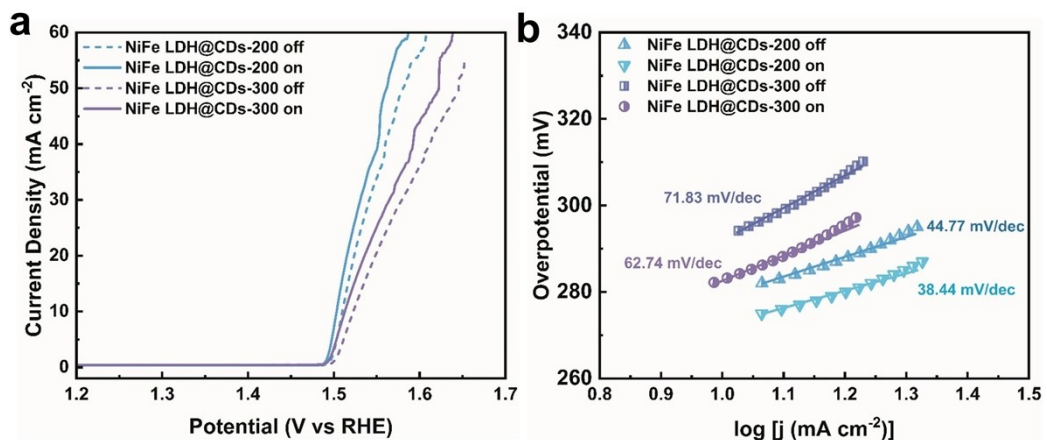


Fig. S9. OER LSV curves (a) and Tafel plots (b) of NiFe LDH@CDs-200 and NiFe LDH@CDs-300 in 1 M KOH with 95% iR-compensation.

Tab. S2. Summary of the overpotential and Tafel slope of Ni-based LDH catalysts

Catalysts	Electrode	Overpotential (10 mA cm ⁻²)	Overpotential (25 mA cm ⁻²)*	Tafel slope (mV dec ⁻¹)	Electrolyte	Reference
NiFe LDH@CDs-200	Glassy carbon	279 mV 273 mV (light on)	303 mV 291 mV (light on)	44.77 38.44 (light on)	1 M KOH	This work
CoNi LDH	Glassy carbon	270 mV	~293 mV	48.7	1 M KOH	[1]
Nanopore-rich NiFe LDH	Glassy carbon	278 mV	-	75	1 M KOH	[2]
Fe-doped NiCo LDH	Glassy carbon	260 mV	~310 mV	70	1 M KOH	[3]
Ru-doped NiFe LDH	Glassy carbon	246 mV	~305 mV	67.2	1 M KOH	[4]
NiFeCo LDH/ Carbon Fiber	Glassy carbon	249 mV	~275 mV	42	1 M KOH	[5]
u-Ni ₇₀ Fe ₃₀ LDH	Copper foil	260 mV	~310 mV	55.6	1 M KOH	[6]
r-NiFe LDH	Nickle foam	320 mV (20 mA cm ⁻²)	~335 mV	80	1 M KOH	[7]
CQDs/NiFe LDH	Glassy carbon	235 mV	~255 mV	30	1 M KOH	[8]
NCD@NiFe LDH	Carbon cloth	252 mV	-	49.8	1 M KOH	[9]
NiCo LDH/Mxene quantum dots	Glassy carbon	316 mV	~360 mV	79	1 M KOH	[10]
N-GQDs/NiFe LDH	Glassy carbon	279 mV (20 mA cm ⁻²)	~295 mV	47	1 M KOH	[11]
NiFe LDH/Co ₃ O ₄	Nickle foam	190 mV	~205 mV	34.6	1 M KOH	[12]

*: The estimated value directly calculated from the LSV curve

Tab. S3. Detail information about EIS fitting data

	NiFe LDH	NiFe LDH@CDs-50	NiFe LDH@CDs-100	NiFe LDH@CDs-200
R_s	4.292 Ω	4.55 Ω	4.185 Ω	4.606 Ω
R_{if}	20.12 Ω	13.54 Ω	13.33 Ω	11.89 Ω
CPE1-T	3.3635×10 ⁻⁵	2.2888×10 ⁻⁵	1.2218×10 ⁻⁵	2.7686×10 ⁻⁵
CPE1-P	0.8002	0.81410	0.88957	0.774
R_{ct}	25.70 Ω	19.80 Ω	17.43 Ω	15.90 Ω
CPE2-T	6.6556×10 ⁻⁴	3.0499×10 ⁻⁴	8.0759×10 ⁻⁵	2.5746×10 ⁻⁴
CPE2-P	0.83995	0.90163	0.8582	0.8199

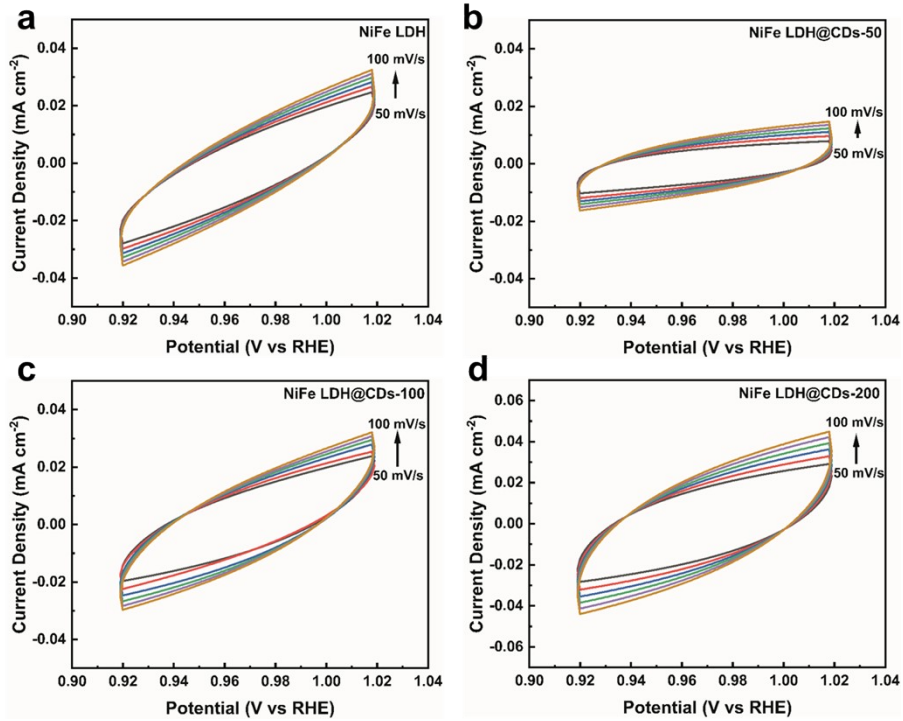


Figure S10 . CV curves with a gradient scan rate of NiFe LDH (a), NiFe LDH@CDs-50 (b), NiFe LDH@CDs-100 (c) and NiFe LDH@CDs-200 (d) in the region of $0.918 \sim 1.018$ V vs RHE.

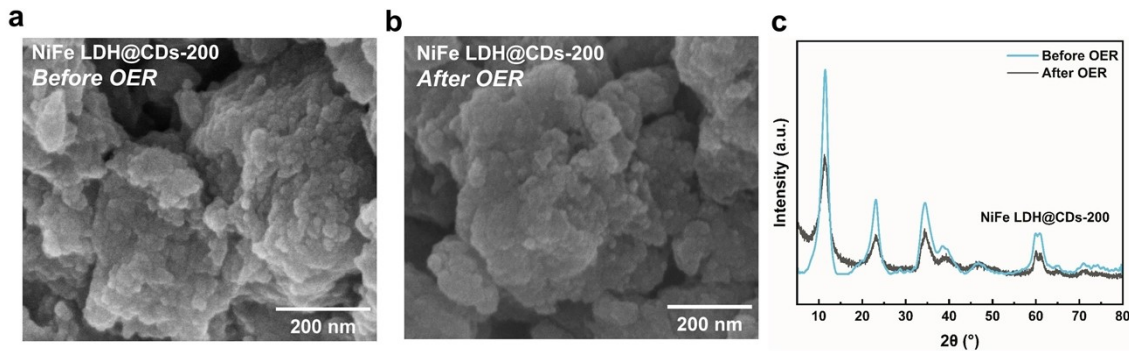


Figure S11. SEM images of NiFe LDH@CDs-200 before (a) and after (b) OER at 10 mA cm^{-2} for 6 h . (c) XRD patterns of NiFe LDH@CDs-200 before and after OER process.

Reference

1. Y. Ma, K. Wang, Y. Chen, X. Yang, S. Zhao, K. Xi, S. Xie, S. Ding and C. Xiao, *Int. J. Hydrogen Energy*, 2019, **44**, 20085-20092.
2. Q. Wen, S. Wang, R. Wang, D. Huang, J. Fang, Y. Liu and T. Zhai, *Nano Res.* 2023, **16**, 2286-2293.
3. Y. Shi, J. Li, B. Zhang, S. Lv, T. Wang and X. Liu, *Appl. Surf. Sci.*, 2021, **565**, 150506
4. Y. Yang, W. Wang, Y. Yang, P. Guo, B. Zhu, K. Wang, W. Wang, Z. He and Z. Liu, *J. Electrochem. Soc.*, 2022, **169**, 024503.
5. Y. Lin, H. Wang, C. Peng, L. Bu, C. Chiang, K. Tian, Y. Zhao, J. Zhao, Y.G. Lin, J. Lee and L. Gao, *Small*, 2020, **16**, e2002426.
6. H. Yang, S. Luo, Y. Bao, Y. Luo, J. Jin and J. Ma, *Inorg. Chem. Front.*, 2017, **4**, 1173-1181.
7. X. Hou, J. Li, J. Zheng, L. Li and W. Chu, *Dalton Trans.*, 2022, **51**, 13970-13977.
8. D. Tang, J. Liu, X. Wu, R. Liu, X. Han, Y. Han, H. Huang, Y. Liu, Z. Kang, *ACS Appl. Mater. Interfaces*, 2014, **6**, 7918-7925.
9. Z. Hu, D. Zhang, C. Sun, C. Song and D. Wang, *Electrochim. Acta*, 2021, **391**, 138932.
10. L. Song, X. Zhang, X. Du, S. Zhu, Y. Xu and Y. Wang, *Phys. Chem. Chem. Phys.*, 2022, **24**, 24902-24909.
11. Q. Dong, C. Shuai, Z. Mo, Z. Liu, G. Liu, J. Wang, Y. Chen, W. Liu, N. Liu and R. Guo, *New J. Chem.*, 2020, **44**, 17744-17752.
12. J. Lv, L. Wang, R. Li, K. Zhang, D. Zhao, Y. Li, X. Li, X. Huang and G. Wang, *ACS Catal.*, 2021, **11**, 14338-14351.